Open Access

ORIGINAL ARTICLE

Prostate Cancer

Secreted protein acidic and rich in cysteine (SPARC) induces epithelial-mesenchymal transition, enhancing migration and invasion, and is associated with high Gleason score in prostate cancer

Fernanda López-Moncada, María José Torres, Enrique A Castellón, Héctor R Contreras

Secreted protein acidic and rich in cysteine (SPARC) is a matricellular protein highly expressed in bone tissue that acts as a chemoattractant factor promoting the arrival of prostate cancer (PCa) cells to the bone marrow. However, the contribution of SPARC during the early stages of tumor progression remains unclear. In this study, we show that SPARC is highly expressed in PCa tissues with a higher Gleason score. Through stable knockdown and overexpression of SPARC in PC3 and LNCaP cells, respectively, here we demonstrate that endogenous SPARC induces the epithelial-mesenchymal transition (EMT), decreasing E-cadherin and cytokeratin 18 and increasing N-cadherin and vimentin. Moreover, SPARC induces the expression of EMT regulatory transcription factors Snail family transcriptional repressor 1 (Snail), Snail family transcriptional repressor 2 (Slug), and zinc finger E-box binding homeobox 1 (Zeb1). In addition, SPARC knockdown in PC3 cells decreases migration and invasion *in vitro*, without modifying cell proliferation. Our results indicate that SPARC might facilitate tumor progression by modifying the cellular phenotype in cancer cells.
Asian Journal of Andrology (2019) 21, 557–564; doi: 10.4103/aja.aja_23_19; published online: 23 April 2019

INTRODUCTION

Prostate cancer (PCa) is the fifth leading cause of death by cancer in men worldwide.[1] Life expectancy is directly related to the appearance of metastasis in this disease. Metastasis is a process in which tumor cells detach from the primary tumor, escape to the circulation and invade distant organs to form secondary tumors. Despite advances in diagnosis and therapies, poor clinical prognosis remains for patients with metastasis. When the disease is confined to the prostate, 5-year survival is 99%; however, when metastasis arises, the 5-year survival falls to 28%.[2,3]

One factor that promotes metastatic progression of PCa cells is secreted protein acidic and rich in cysteine (SPARC). SPARC, also known as basement membrane-40 (BM-40) and osteonectin, is a matricellular glycoprotein that promotes collagen deposition in the stroma.[4,5] Consequently, SPARC is highly expressed in tissues with high turnover of the extracellular matrix, such as bone tissue, healing wounds, and malign tumors.[6] In addition, SPARC regulates numerous biological processes important for tumor progression, such as cell proliferation, differentiation, adhesion, migration, and angiogenesis.[7]

In tumors, SPARC can be secreted from cancer cells, the surrounding stromal cells, or both.[8–10] High expression of SPARC is related to tumor progression in melanoma, pancreatic cancer, breast cancer, glioma, and others.[10–13] In PCa, evidence shows SPARC promoting both pro- and anti-tumor properties. Exogenous SPARC, present in bone extracts or purified, promotes tumor progression by acting as chemoattractant that directs tumor cell homing to the bone.[14,15] However, exogenous SPARC also inhibits tumor progression by suppressing migration[16] and tumor cell growth.[16–18] More recently, it has been found that SPARC upregulates canonical transcription factors that induce epithelial-mesenchymal transition (EMT), such as Snail family transcriptional repressor 1 (Snail) and Snail family transcriptional repressor 2 (Slug), in melanoma and non-small cell lung cancer.[19–21] EMT is a transdifferentiation program crucial for metastasis because cells undergoing EMT change their polarity, lose cell-cell contact, migrate, and invade the tumor stroma.[22,23] In cancer cells, EMT activation can be induced and maintained by secreted proteins, such as cytokines and growth factors present in the tumor microenvironment, through paracrine or autocrine mechanisms.[24] Because SPARC upregulates canonical EMT transcription factors (EMT-TFs), we propose that endogenous SPARC induces molecular and functional changes associated with EMT, in early stages of tumor development, thus promoting metastatic progression. In this study, we show that SPARC is expressed in PCa primary tumors with higher Gleason scores (GSs). Through silencing and overexpression of SPARC in PCa, we demonstrate that SPARC induces the EMT program in PCa, increasing their motility and invasive capacities in an autocrine manner.

MATERIALS AND METHODS

Tissue micro arrays (TMAs)

Formalin-fixed and paraffin-embedded samples from patients

Department of Basic and Clinic Oncology, Faculty of Medicine, University of Chile, Santiago 8389100, Chile.
Correspondence: Dr. HR Contreras (hcontrer@med.uchile.cl)

diagnosed with PCa were obtained after radical prostatectomy surgery at the Clinical Hospital of the University of Chile, Santiago, Chile. All samples were evaluated by an expert pathologist and classified according to their GS: samples with a score of 6 were classified as low GS, samples with a score of 7 were classified as intermediate GS, and samples scored from 8 to 10 were classified as high GS. From the tissue specimens collected, we constructed two TMAs that contained 1-mm diameter cores of samples, including 23 samples of low GS, 59 samples of intermediate GS, and 26 samples of high GS, plus 12 samples of benign prostatic hyperplasia (BPH). This study was approved by the Bioethics Committees of the Faculty of Medicine and the Clinical Hospital of the University of Chile, and all patients provided informed consent.

Immunohistochemistry (IHC)

Tissue sections obtained from the TMAs were processed and stained in an automated IHC stainer (Benchmark GX, Ventana, Tucson, AZ, USA), according to standard procedures. Briefly, samples were dewaxed, rehydrated, and incubated for 30 min at 95°C in antigen retrieval buffer (citrate buffer, pH 8.0). After blocking, sections were probed with a specific antibody against SPARC (1:100, 335500, Life Technologies, Carlsbad, CA, USA) and nuclei were stained with hematoxylin (Scytek laboratories, Logan, UT, USA). Digital images were obtained using a Leica DM2500 microscope (Leica, Wetzlar, Germany) and 3,3'-diaminobenzidine (DAB) signal was quantified using the software ImageJ 1.51w (NIH, Bethesda, MD, USA), with the IHC toolbox plugin.

Cell culture

All cell lines were purchased from the American Type Culture Collection (ATCC, Manassas, VA, USA). LNCaP clone FGC (CRL1740) and 22Rv1 (CRL2505) cells were maintained in Roswell Park Memorial Institute (RPMI) 1640 media (GIBCO, Life Technologies). DU145 (HTB81) and PC3 (CRL1435) cells were maintained in Dulbecco's modified Eagle's medium (DMEM) F12 media (GIBCO). Both culture media were supplemented with 10% fetal bovine serum (FBS; Mediatech, Manassas, VA, USA), streptomycin-penicillin and amphotericin B (Corning Inc., Corning, NY, USA). All cell cultures were maintained at 37°C, in a humidified atmosphere with 5% CO_2.

Lentiviral transduction

Knockdown cells for SPARC were obtained through transduction with lentiviral vectors containing short hairpin RNA (shRNA) against SPARC (pLenti-U6-shRNA [h SPARC]-Rsv[GFP-Puro]), or shRNA scramble as control (pLenti-U6-shRNA [Neg-control]-Rsv[GFP-Puro]). To overexpress SPARC, cells were transduced with lentivirus containing the SPARC sequence coupled to a HA tag (pLenti-suCMV[h SPARC-HA]-Rsv[GFP-Puro]) or the empty vector as control (pLenti-suCMV[Null-control]-Rsv[GFP-Puro]). All lentiviruses were purchased from Gen Target Inc. (San Diego, CA, USA) and cells were infected using a standard procedure. Briefly, 7.5×10^4 cells per well were seeded in 6-well plates. After 24 h, cells were incubated with lentiviral particles at a multiplicity of infection of three, plus 5 μg ml^{-1} polybrene (Sigma-Aldrich, St. Louis, MO, USA) in 1 ml of culture media for 24 h. Later, cells integrating the vectors were selected using 2 μg ml^{-1} puromycin (Sigma-Aldrich) for 24 h.

Western blot

Whole-cell protein was extracted using radioimmunoprecipitation assay (RIPA) buffer with Complete Mini, ethylenediaminetetraacetic acid (EDTA)-free protease inhibitor cocktail (Roche, Indianapolis, IN, USA). Next, 50 μg protein was loaded and separated by sodium dodecyl sulfate-polyacrylamide gel electrophoresis (SDS-PAGE) and transferred to a nitrocellulose membrane. Blots were blocked with 5% bovine serum albumin (BSA) in Tris-buffered saline (TBS) with 0.2% Tween and incubated overnight with primary antibodies diluted in blocking buffer. After washing, bound primary antibodies were detected with horseradish peroxidase (HRP)-conjugated secondary antibodies and revealed with an enhanced chemiluminescence detection kit for HRP (EZ-ECL, Biological Industries, Cromwell, CT, USA). The antibodies used in this work were: anti-SPARC (1:500, sc-25574, Santa Cruz, Dallas, TX, USA), anti-hemagglutinin (HA; 1:1000, H6908, Sigma-Aldrich), anti-zinc finger E-box binding homeobox 1 (Zeb1; 1:1000, 14974182, eBioscience, Thermo Fisher, Waltham, MA, USA), anti-Snail (1:500, sc-393172, Santa Cruz), anti-Slug (1:500, sc-166479, Santa Cruz), anti-E-cadherin (1:1000, 610181, BD Transduction Laboratories, San Jose, CA, USA), anti-N-cadherin (1:1000, 333900, Life Technologies), anti-Vimentin (1:2000, ab8978, AbCam, Cambridge, UK), anti-Actin (1:5000, MP Biomedicals, Santa Ana, CA, USA), anti-mouse HRP (1:10000, Jackson Immunoresearch, West Grove, PA, USA), and anti-rabbit HRP (1:10000, Jackson Immunoresearch).

RNA extraction and quantitative real-time reverse transcriptase PCR (RT-qPCR)

Total RNA was extracted from cells using TRIzol (Ambion, Life Technologies). Three thousand nanograms of cDNA was synthetized using the kit cDNA Affinity Script QPCR (Agilent Technologies, Santa Clara, CA, USA) and 100 ng of cDNA was amplified by qPCR using the kit Brilliant II SYBR Green qPCR Master Mix (Agilent Technologies). The housekeeping gene pumilio RNA binding family member 1 (*PUM1*) was used as normalizer and the results were analyzed using the ΔΔCt method. The primer sets used for the qPCRs are detailed in **Table 1**.

Table 1: The primer sets used for the quantitative polymerase chain reactions

Gene name (protein common name)	Abbreviation	Forward primer	Reverse primer
Secreted protein acidic and rich in cysteine (SPARC)	*SPARC*	5'-AAC CGA AGA GGA GGT GGT-3'	5'-GCA AAG AAG TGG CAG GAA GA-3'
Cadherin 1 (E-cadherin)	*CDH1*	5'-GAA CGC ATT GCC ACA TAC AC-3'	5'-ATT CGG GCT TGT TGT CAT TC-3'
Cadherin 2 (N-cadherin)	*CDH2*	5'-GGA CAG TTC CTG AGG GAT CA-3'	5'-GGA TTG CCT TCC ATG TCT GT-3'
Vimentin (Vimentin)	*VIM*	5'-GCC AAG GCA AGT CGC G-3'	5'-CAT TTC ACG CAT CTG GCG-3'
Keratin 18 (Cytokeratin 18)	*KRT18*	5'-ACA GAG TGA GGA GCC TGG AGA CCG A-3'	5'-CAG TAT TTG CGA AGA TCT GAG CCC TC-3'
Zinc finger e-box binding homeobox 1 (Zeb1)	*ZEB1*	5'-TTC ACA GTG GAG AGA AGC CA-3'	5'-GCC TGG TGA TGC TGA AAG AG-3'
Snail family transcriptional repressor 1 (Snail)	*SNAI1*	5'-TTC AGC AGC CCT ACG ACC AG-3'	5'-GCC TTT CCC ACT GTC CTC ATC-3'
Snail family transcriptional repressor 2 (Slug)	*SNAI2*	5'-CTC CAT TCC ACG CCC AGC TAC-3'	5'-AGC CAC TGT GGT CCT TGG AG-3'
Matrix metallopeptidase 2 (Matrix metalloproteinase-2)	*MMP-2*	5'-AAG CCC AAG TGG GAC AAG AA-3'	5'-ACT TGG AAG CGC AGA GCA AA-3'
Matrix metallopeptidase 7 (Matrix metalloproteinase-7)	*MMP-7*	5'-TGG GAC ATT CCT CTG ATC CT-3'	5'-TGA ATG GAT GTT CTG CCT GA-3'
Pumilio RNA binding family member 1 (Pumilio homolog 1)	*PUM1*	5'-CGG TCG TCC TGA GGA TAA AA-3'	5'-CGT ACG TGA GGC GTG AGT AA-3'

Indirect immunofluorescence and fluorescent staining

Cells were seeded in 12-mm coverslips at a confluence of 50%. After 24 h, cells were fixed in 4% paraformaldehyde for 30 min, permeabilized with 0.1% Triton X-100 in PBS for 10 min, washed, and blocked with 3% BSA in PBS for 30 min. Cells were incubated overnight with primary antibodies against SPARC (1:100, sc-25574, Santa Cruz), Zeb1 (1:50, sc-25388, Santa Cruz) or Ki67 (1:50, sc-15402, Santa Cruz), washed and incubated for 45 min with secondary antibody Alexa Fluor 594 (1:500, A21207, Life Technologies). 4′,6-diamidino-2-phenylindole (DAPI; 1:10000, sc3598, Santa Cruz) and Phalloidin (50 µg ml^{-1}, P-1951, Sigma-Aldrich) were used for nuclear and cytoplasmic staining, respectively. Cell area and circularity were quantified using the software ImageJ 1.51w.

Wound healing assay

Cells were seeded in 24-well plates and cultured on confluence. A scratch was made with a pipette tip and the wound was photographed every 12 h for 3 days. Wound area was quantified using the software ImageJ 1.51w.

Transwell migration assay

For transwell migration assay, 5×10^4 cells per well were seeded in the upper chamber of a 96-well CytoSelect™ (Cell Biolabs, San Diego, CA, USA) plate with 8-µm pore membranes. Cells in the upper chamber were kept in culture media without FBS, whereas in the lower chamber, culture media with 10% FBS was placed as chemoattractant. After 24 h, transmigrated cells were resuspended and dyed with CyQuant® GR Dye (Cell Biolabs). Fluorescence at 485/528 nm was quantified in a BioTek Synergy HT plate reader (BioTek, Winooski, VT, USA).

In vitro invasion assay

Invasion assay was performed in a 96-well CytoSelect™ (Cell Biolabs) plate with 8-µm pore membranes coated with the basement membrane, following the same protocol used for the transwell migration assay described above.

MTT viability assay

Cell viability was assessed using 3-(4,5-dimethylthiazol-2-yl)-2,5-diphenyltetrazolium bromide (MTT). For this, 1×10^4 cells per well were seeded in a 48-well plate. After 24 h, 48 h and 72 h, cells were washed in PBS. Then, 100 ml of MTT working solution (15 µl MTT [5 mg ml^{-1}] in 500 µl Locke solution) was added and cells were incubated for 3 h at 37°C. Afterward, the solution was discarded, formazan crystals were resuspended in 100 µl dimethyl sulfoxide and the absorbance at 550 nm was measured in a BioTek Synergy HT plate reader (BioTek).

Trypan blue exclusion test

For the trypan blue exclusion test, 5×10^4 cells per well were seeded in 12-well plates and cell growth was monitored every 24 h for 3 days, by counting the total number of viable cells per well. For this, cells were detached with trypsin and resuspended in 1 ml culture media. Next, 10 µl trypan blue (0.4%; Sigma-Aldrich) was added to 10 µl of cell suspension and 10 µl of this mix was loaded in a hemocytometer (Paul Marienfeld GmbH & Co. KG, Lauda-Königshofen, Germany). Only viable (nonstained) cells were considered for the count.

Statistical analyses

Data analysis was performed using GraphPad Prism 6.0 (GraphPad Software, La Jolla, CA, USA). For TMA analysis, data distribution was evaluated with the D'Agostino-Pearson normality test and differences between groups was analyzed with the Kruskal–Wallis test. In all other experiments, data are expressed as mean ± standard deviation,

of at least three independent experiments. For continuous data, Mann–Whitney U test, Student's *t*-test, and one-way ANOVA or two-way ANOVA were used to analyze differences between groups. In all cases, $P \leq 0.05$ was considered statistically significant.

Ethical and safety considerations

All procedures were approved by the Ethics Committee for Research on Human Beings and the Risk Prevention and Biosafety Unit of the Faculty of Medicine of the University of Chile.
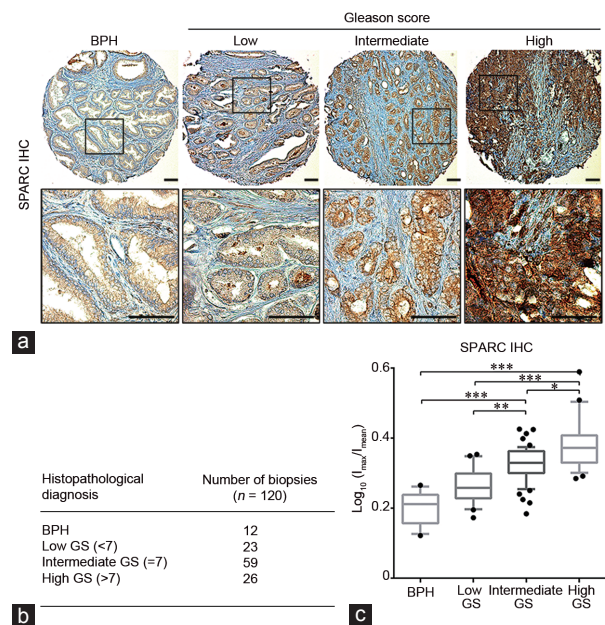
RESULTS

Expression of SPARC in PCa samples is associated with high GS

To evaluate SPARC expression in human PCa samples, two TMAs including prostate tissue specimens of 120 patients were constructed and immunohistochemistry staining of SPARC was performed (**Figure 1a** and **1b**). PCa specimens present positive intracellular staining for SPARC (**Figure 1a**). Furthermore, quantification of DAB staining (**Figure 1c**) revealed that SPARC expression is increased in samples of intermediate and high GS compared with those of nonneoplastic prostate disease (BPH) ($P \leq 0.001$, Kruskal–Wallis test) or PCa samples of low GS ($P \leq 0.01$, Kruskal–Wallis test).

Stable silencing and overexpression of SPARC change morphological features in PCa cell lines

Because SPARC showed high expression in the more aggressive PCa, we aimed to determine the biological effects of SPARC *in vitro*, modifying its expression in PCa cell lines. For this, we first determined the base levels of SPARC in different PCa cell lines. Four frequently-used cell lines were selected: 22Rv1, LNCaP, DU145, and PC3. PC3 cells have the highest expression of SPARC mRNA and protein

Histopathological diagnosis	Number of biopsies ($n = 120$)
BPH	12
Low GS (<7)	23
Intermediate GS (=7)	59
High GS (>7)	26

Figure 1: Expression of SPARC in biopsy samples of patients with PCa. (**a**) Representative images of IHC against SPARC in TMAs of samples of BPH and PCa of low, intermediate, and high GS. Lower row corresponds to a magnification of the upper images. Scale bars = 100 µm. (**b**) Number of biopsy samples analyzed per group. (**c**) Quantification of DAB signal. The box-plots depict the intensity SPARC signal in each group. Dots outside the box-plot depict the outliers. *$P \leq 0.05$, **$P \leq 0.01$, and ***$P \leq 0.001$ (Kruskal–Wallis test). SPARC: secreted protein acidic and rich in cysteine; TMAs: tissue micro arrays; PCa: prostate cancer; IHC: immunohistochemistry; BPH: benign prostatic hyperplasia; GS: Gleason score; DAB: 3,3'-diaminobenzidine.

(**Figure 2a** and **2b**). Conversely, 22Rv1, LNCaP and DU145 cells have very low SPARC expression. Based on this, we chose the PC3 cell line to knock down SPARC through transduction with lentiviral vectors expressing a shRNA directed against SPARC. The LNCaP cell line was used to overexpress SPARC by transduction with lentiviral vectors expressing the SPARC sequence. Western blot (**Figure 2c**), RT-qPCR (**Figure 2d**) and immunofluorescence (**Figure 2e**) confirmed the changes in the intracellular levels of SPARC ($P \leq 0.001$, one-way ANOVA). In addition, morphological features of cells with SPARC silencing and overexpression were assessed. PC3 shScramble cells have a fusiform shape, while PC3 ShSPARC cells are more circular and bigger ($P \leq 0.001$, Mann–Whitney U test), which is consistent with an epithelial morphology. Conversely, LNCaP cells with overexpression of SPARC are smaller ($P = 0.017$, Mann–Whitney U test), although

the circularity does not change ($P = 0.779$, Mann–Whitney U test) (Figure **2f–2h**).

SPARC induces EMT in PCa cell lines

To determine whether SPARC could modulate the cellular phenotype, classical EMT markers, the cell-cell adhesion molecules E-cadherin and N-cadherin and the intermediate filaments vimentin and cytokeratin 18 were evaluated in the established cell lines. Knockdown of SPARC in PC3 cells resulted in increased E-cadherin ($P = 0.013$, Student's t-test) and cytokeratin 18 ($P \leq 0.01$, Student's t-test), accompanied by a decrease in N-cadherin and vimentin ($P \leq 0.001$, Student's t-test). Conversely, overexpression of SPARC in LNCaP cells downregulated E-cadherin and cytokeratin 18 ($P \leq 0.001$, Student's t-test), and upregulated vimentin ($P = 0.019$, Student's t-test). Although SPARC overexpression
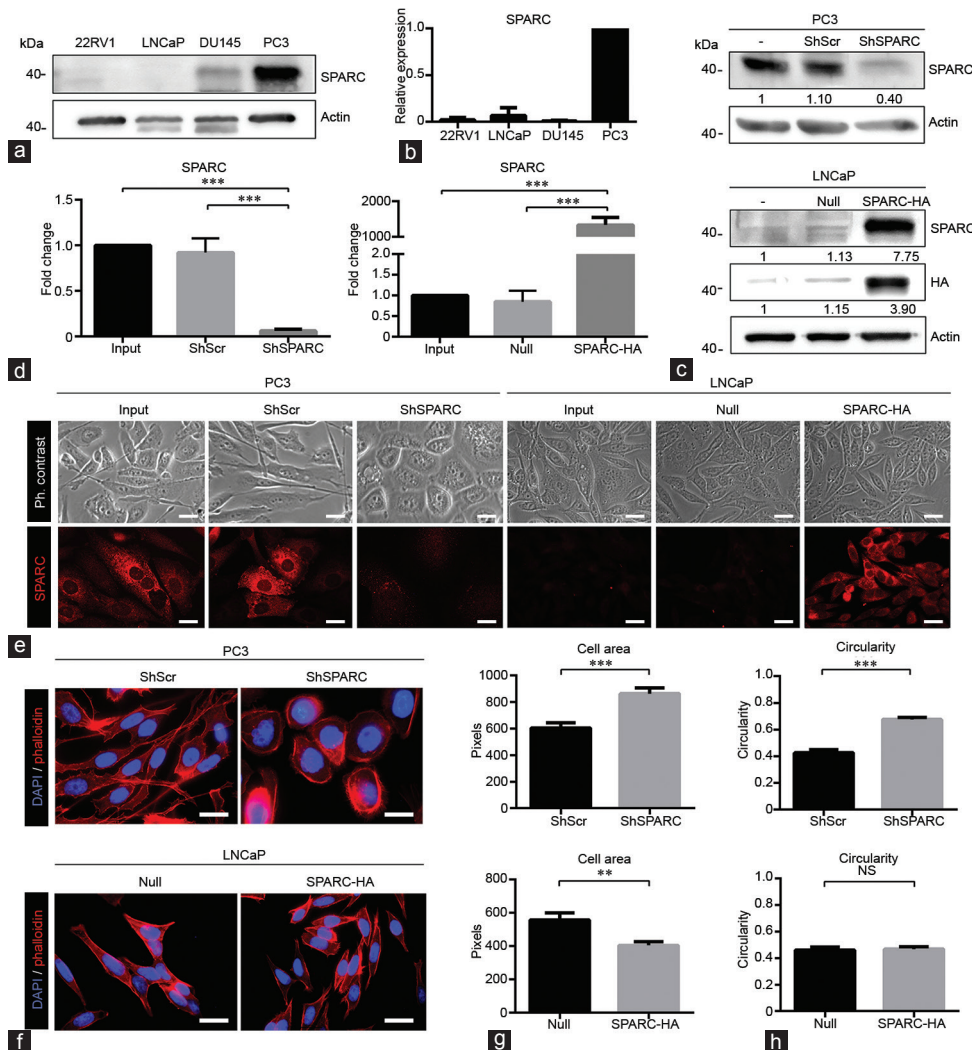
Figure 2: Basal expression, silencing, and overexpression of SPARC in PCa cell lines. (**a**) Representative image of western blot against SPARC in PCa cell lines 22Rv1, LNCaP, DU145 and PC3. (**b**) RT-qPCR of SPARC in PCa cell lines. ΔΔCt was obtained after normalizing to PUM1 and PC3 cell lines ($n = 3$). (**c** and **d**) PC3 cells were stable transduced with shRNA against SPARC (ShSPARC) or scramble (ShScr). LNCaP cells were stable transduced with SPARC sequence (SPARC-HA) or an empty vector (Null). Parental cells (Input) were used as control. (**c**) Representative images of western blot against SPARC in the different cell lines produced. Quantification of optic density was normalized to β-actin and parental cells, numbers show median ($n = 3$). (**d**) SPARC mRNA expression assessed through RT-qPCR ($n = 3$); ***$P \leq 0.001$ (one-way ANOVA). (**e**) Representative images of phase contrast and immunofluorescence against SPARC in transduced and parental cell lines. (**f**) Representative images of transduced PC3 and LNCaP cell stained with DAPI and phalloidin. Scale bars = 20 μm in **e** and **f**. (**g**) Cell area and (**h**) circularity of transduced PC3 and LNCaP cells stained with DAPI and phalloidin ($n = 50$); **$P = 0.017$; ***$P \leq 0.001$, NS: not significant, $P > 0.05$ (Mann–Whitney U test). SPARC: secreted protein acidic and rich in cysteine; PUM1: pumilio RNA binding family member 1; ANOVA: analysis of variance; RT-qPCR: quantitative real-time reverse transcriptase PCR; ShSPARC: shRNA against SPARC; ShScr: shRNA against scramble; DAPI: 4',6-diamidino-2-phenylindole.

increased N-cadherin expression, it was not possible to quantify these changes because parental and null LNCaP cells do not show N-cadherin expression by RT-qPCR or western blot (**Figure 3a** and **3c**). Together, the changes in EMT markers expression indicate that SPARC induces EMT in PCa cell lines. Because the changes in protein expression that occur during the EMT are regulated by transcriptional factors that inhibit the transcription of genes associated with epithelial phenotype and induce the transcription of mesenchymal genes, we assessed whether SPARC can modify the expression levels of the EMT-TFs Zeb1, Snail, and Slug. SPARC knockdown in PC3 cells decreased the mRNA of the transcription factors Zeb1 ($P \le 0.001$, Student's *t*-test), Snail ($P = 0.026$, Student's *t*-test), and Slug ($P \le 0.001$, Student's *t*-test) (**Figure 3d**). However, at protein level, only decrease of Zeb1 was observed ($P \le 0.001$, Student's *t*-test) (**Figure 3b**). Conversely, the stable overexpression of SPARC in LNCaP cells increased the expression of Zeb1 ($P \le 0.001$, Student's *t*-test), Snail ($P = 0.017$, Student's *t*-test), and Slug ($P = 0.026$, Student's *t*-test), both at the mRNA and protein levels (**Figure 3b** and **3d**). As active EMT-TFs are localized in the nucleus, Zeb1 expression, through indirect immunofluorescence, was also evaluated. As expected, in normal PC3 cells and LNCaP cells with SPARC overexpression, a strong Zeb1 signal was observed into the nuclei, whereas in normal LNCaP and in PC3 cells knockdown for SPARC, only a diffuse cytoplasmic signal was observed (**Figure 3e**).

SPARC does not induce changes in the proliferation of PCa cells
Given that SPARC upregulates the expression of EMT-TFs, which can

directly inhibit proliferation, the effect of SPARC on cell proliferation in PCa cell lines was evaluated. We observed that neither silencing nor overexpression of SPARC in PCa cells modifies *in vitro* proliferation, evaluated by three different methods: MTT ($P = 0.993$, two-way ANOVA), Trypan Blue exclusion test ($P = 0.999$, two-way ANOVA), and immunofluorescence against Ki67 ($P = 0.842$, one-way ANOVA) (**Figure 4**).

SPARC increases the motility and in vitro invasive capacity of PCa cells
Because high motility is one of the distinctive features of mesenchymal cells, we evaluated whether SPARC-induced mesenchymal phenotype is accompanied by an increase in cell motility. We assessed the motility capacities of PCa cells with SPARC knockdown and overexpression through a wound closure test. Silencing of SPARC in PC3 decreased the motility of these cells ($P \le 0.001$, two-way ANOVA), while the overexpression of SPARC in LNCaP cells increased it ($P \le 0.001$, two-way ANOVA) (**Figure 5a** and **5b**). To confirm these findings, we performed a migration test with a modified Boyden chamber, using FBS as chemoattractant. As expected, cells expressing SPARC showed a high ability to transmigrate through the chamber pores in response to the chemoattractant stimulus (PC3 cells: $P \le 0.01$; LNCaP cells: $P = 0.018$, Student's *t*-test) (**Figure 5c**).

To determine whether SPARC also increases the invasive capacity, a modified Boyden chamber coated in basement membrane was used. SPARC-knockdown PC3 cells showed lower ability to invade through the matrix than normal PC3 cells ($P = 0.047$, Student's *t*-test)
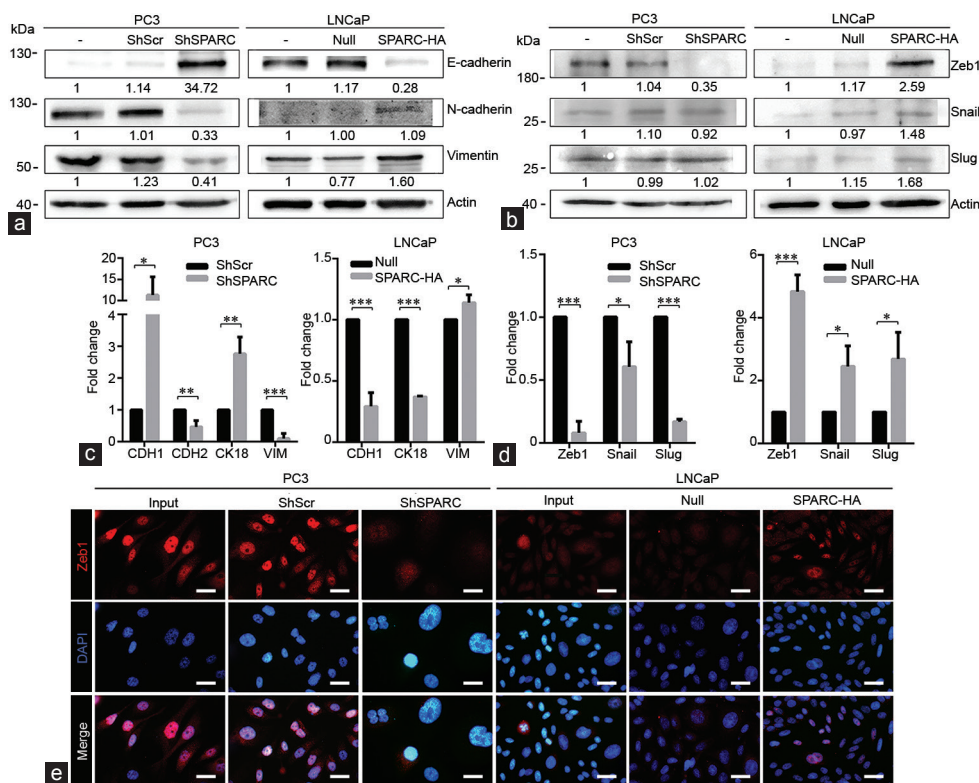
Figure 3: Expression of EMT markers and EMT-TFs in PCa cell lines with SPARC knockdown and overexpression. (**a**) Western blot of EMT markers E-cadherin, N-cadherin and vimentin and (**b**) EMT-TFs Zeb1, Snail and Slug in PC3 cells transduced with shRNA against SPARC, LNCaP cells transduced with the SPARC sequence and its respective controls. Quantification of optic density was normalized to β-actin and parental cells, numbers show median ($n = 3$). Relative mRNA expression of (**c**) EMT markers and (**d**) EMT-TFs, assessed by RT-qPCR ($n = 3$); *$P \le 0.05$, **$P \le 0.01$, and ***$P \le 0.001$ (Student's *t*-test). (**e**) Representative images of immunofluorescence against Zeb1 in PC3 with SPARC silencing and LNCaP cells with SPARC overexpression and its respective controls. Scale bars = 20 µm. Zeb1: zinc finger E-box binding homeobox 1; EMT: epithelial-mesenchymal transition; EMT-TFs: EMT transcription factors; shRNA: short hairpin RNA; SPARC: secreted protein acidic and rich in cysteine; RT-qPCR: quantitative real-time reverse transcriptase PCR; VIM: Vimentin; ShSPARC: shRNA against SPARC; ShScr: shRNA against scramble; DAPI: 4',6-diamidino-2-phenylindole; Snail: Snail family transcriptional repressor 1; Slug: Snail family transcriptional repressor 2.

(**Figure 5d**), but LNCaP cells with SPARC overexpression showed no changes in their invasive capacity (*P* = 0.435, Student's *t*-test).

Because matrix metalloproteinases (MMPs) are crucial for tumor cell invasion, we evaluated their expression in PCa cells with SPARC silencing and overexpression. SPARC knockdown downregulated MMP-2 and MMP-7 mRNA levels in PC3 cells (*P* < 0.001, Student's *t*-test). However, no changes were observed in the expression of MMP-2 (*P* = 0.102, Student's *t*-test) and MMP-7 (*P* = 0.084, Student's *t*-test) in LNCaP cells with SPARC overexpression (**Figure 5e**).

DISCUSSION

SPARC is a matricellular protein highly expressed in bone tissue and described as a chemoattractant factor that could promote the arrival of PCa cells in the bone marrow.[11,14,15] However, there is no consensus regarding its contribution during the early stages of tumor progression.[7]

In this study, we found that SPARC is expressed in primary tumor biopsies from PCa patients, being high in those of intermediate and high GS. Our results confirm those of Sung *et al.*[8] who found that PCa tissue expresses more SPARC than normal prostate tissue, and of Derosa *et al.*[25] who showed that SPARC is more expressed by poorly-differentiated PCa compared with well-differentiated PCa tumors. Conversely, Shin *et al.*[16] found that normal prostates have a higher intensity of SPARC immunostaining compared with PCa tissue. Because several other studies have linked SPARC expression with both normal and tumor tissue,[7,13] it is clear that SPARC expression varies during cancer progression and might exert different effects in this disease.

In the PCa cell lines studied in this work, we observed that SPARC is highly expressed in PC3 cells compared with the other three PCa cell lines. This result is consistent with the findings of Thomas *et al.*[26] who found that PCa cells obtained from bone metastases such as PC3 have higher expression of SPARC compared with cells obtained from primary tumors or metastasis in other organs. However, because we found that primary tumors of intermediate and high GS also express SPARC, it is possible that this increased expression of SPARC might be acquired during this earlier stage of tumor progression and not once in the bone. To investigate the effects of tumor SPARC in PCa cells, we developed an *in vitro* model of silencing and overexpression of SPARC. In our model, we found that SPARC expression by PCa cells leads to morphological, molecular, and functional changes associated with EMT. Our results are in agreement with recent studies in head and neck cancer and non-small cell lung cancer in which SPARC induces phenotypic and molecular changes associated with EMT.[20,27] The present work is the first report of EMT induction by SPARC in PCa.

In this study, we observed that SPARC knockdown decreases the expression of Zeb1, Snail and Slug at the mRNA level. However, at the protein level, only Zeb1 is downregulated. Snail and Slug can
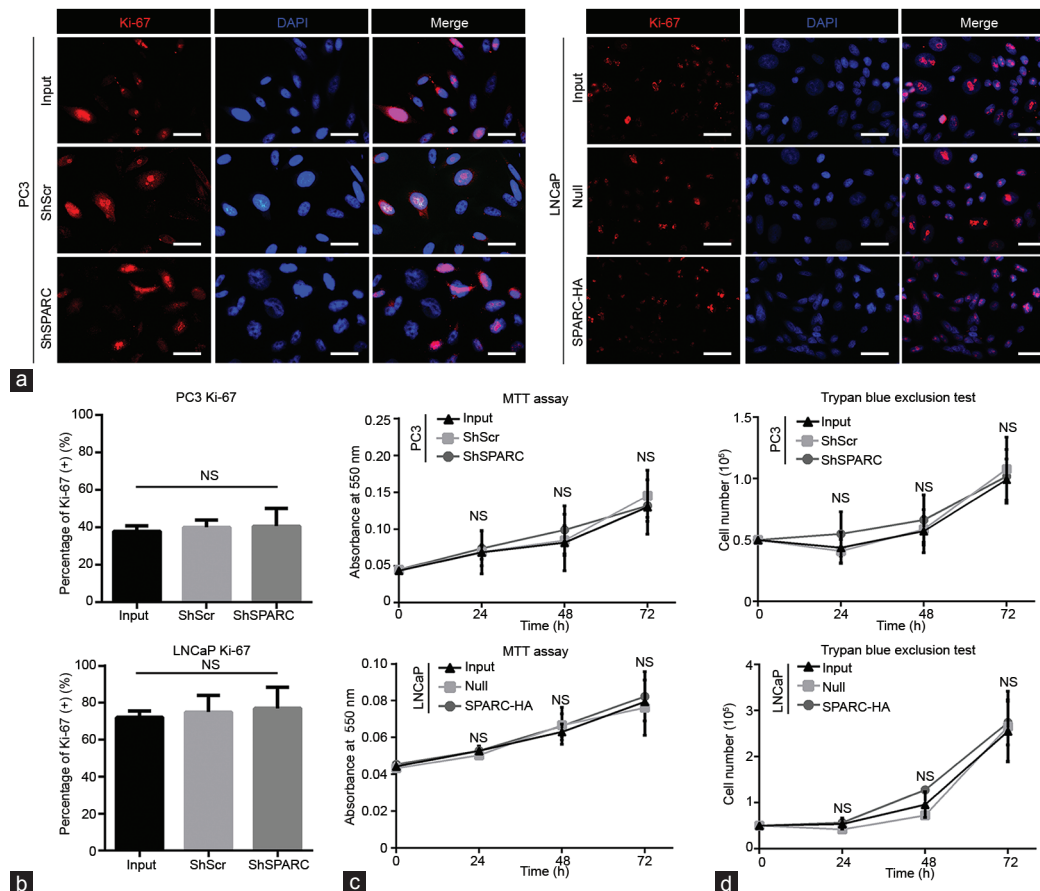
Figure 4: Cell proliferation in prostate cell lines with SPARC knockdown and overexpression. (**a**) Representative images of immunofluorescence against Ki67. Scale bars = 20 mm. (**b**) Quantification of Ki67 positive nuclei, with respect to the total (*n* = 3), NS: not significant, *P*>0.05 (one-way ANOVA). (**c**) MTT cell grow assay. Every 24 h, cells were incubated with MTT and the absorbance at 550 nm was measured (*n* = 5). (**d**) Trypan blue exclusion test. 5 × 10⁴ cells per well were seeded in 12-well plates. Every 24 h, cells were incubated with trypan blue and nonstained cells were counted in a hemocytometer (*n* = 5). NS: not significant, *P* > 0.05 (two-way ANOVA) in **c** and **d**. SPARC: secreted protein acidic and rich in cysteine; ShSPARC: shRNA against SPARC; ShScr: shRNA against scramble; DAPI: 4′,6-diamidino-2-phenylindole; ANOVA: analysis of variance; MTT: 3-(4,5-dimethylthiazol-2-yl)-2,5-diphenyltetrazolium bromide.
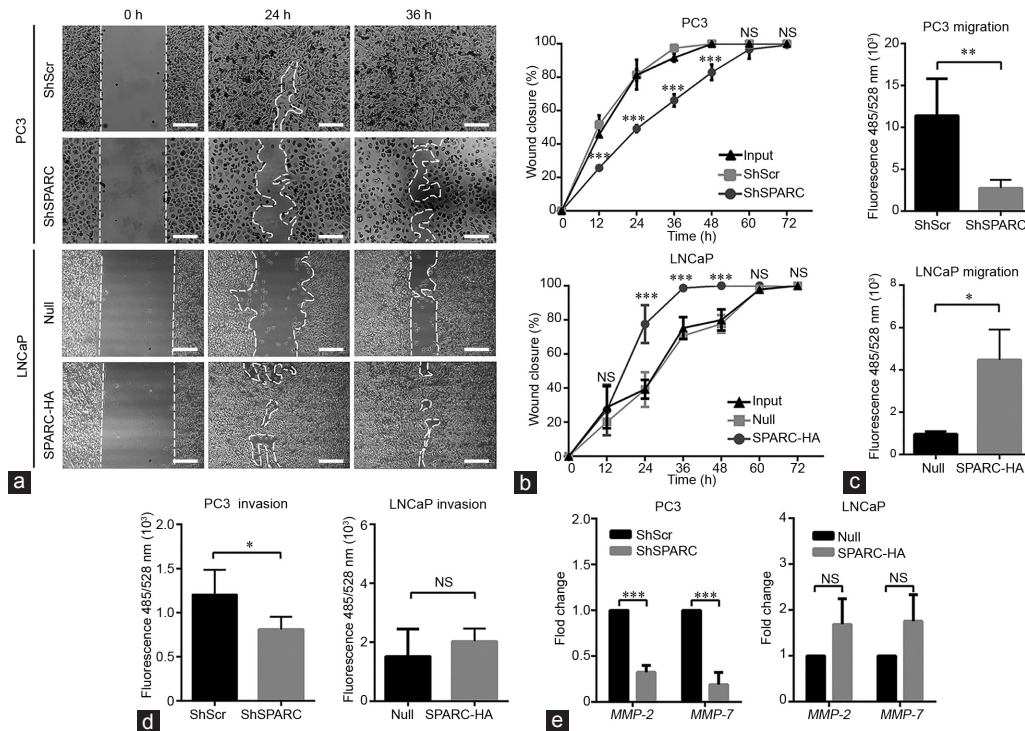
Figure 5: Effects of SPARC on the motility and invasive capacity of prostate cancer cells *in vitro*. (**a**) Representative images of the wound healing assay. Confluent cultures were scratched with a pipette tip and wound closure was monitored every 12 h. Scale bars = 200 μm. (**b**) Wound closure percentage is expressed with respect time 0 (*n* = 3); NS: not significant, $P > 0.05$, ***$P \leq 0.001$ (two-way ANOVA). (**c**) Migration assay performed in a modified Boyden chamber. Transmigrated cells were stained and quantified after 24 h. (**d**) Invasion assay performed in a modified Boyden chamber coated with a basement membrane layer. Invasive cells were stained and quantified after 24 h. (**e**) *MMP-2* and *MMP-7* mRNA expressions were measured by RT-qPCR. *n* = 3 in all cases of **c–e**. NS: not significant, $P > 0.05$, *$P \leq 0.05$, **$P \leq 0.01$, and ***$P \leq 0.001$ (Student's *t*-test). *MMP-2*: matrix metalloproteinases 2; *MMP-7*: matrix metalloproteinases 7; RT-qPCR: quantitative real-time reverse transcriptase PCR; SPARC: secreted protein acidic and rich in cysteine; ShSPARC: shRNA against SPARC; ShScr: shRNA against scramble; ANOVA: analysis of variance.

be translationally regulated,[28,29] which could explain why Snail is downregulated at the mRNA level in PC3 ShSPARC cells, but not at the protein level. In addition, SPARC overexpression upregulates canonical EMT-TFs Snail, Slug and Zeb1, at the mRNA and protein level, which suggests that SPARC could modulate the cellular phenotype through these transcriptional factors. Because tumor cells with knockdown of Zeb1, Snail, and Slug change to an epithelial phenotype, with increased expression of E-cadherin,[30,31] Snail is necessary for SPARC-induced downregulation of E-cadherin in non-small cell lung cancer,[20] and Slug is necessary for SPARC-induced invasion in melanoma,[19] these transcription factors may be necessary for SPARC-induced EMT in PCa. However, it is possible that SPARC may also act through other mechanisms different to the regulation through these transcription factors. For example, because SPARC activates integrins a_vb_3 and a_vb_5,[14] it could promote internalization of E-cadherin through downstream integrin effectors focal adhesion kinase (FAK) and the tyrosine-protein kinase transforming protein Src (v-Src).[32] Furthermore, no reports exist regarding the contribution of Zeb1 in the EMT induced by SPARC. This is relevant because we found that Zeb1 is the EMT-TF presenting the highest variation when overexpressing or silencing SPARC. Moreover, several studies have shown that Zeb1 promotes therapy resistance through EMT-dependent and EMT-independent mechanisms.[33–35] It would be interesting to determine whether SPARC regulates other important aspects of tumor progression through Zeb1, Snail, Slug, or integrin signaling.

Said *et al.*[18] reported that mice knockout for SPARC show fast PCa tumor growth and increased tumor cell proliferation. Similarly, Shin

et al.[16] observed a decrease in PCa cell proliferation in the presence of exogenous SPARC. Conversely, other studies have described either an increase[14] or no change in the proliferative capacities.[15,36,37] In agreement with these last three studies, no changes in proliferation when silencing or overexpressing SPARC were observed. Considering that SPARC induces EMT, it is possible that the effects of SPARC on tumor growth depend on the differential activation of EMT-TFs that activate pro- and anti-proliferative pathways. For example, Zeb1 promotes proliferation via ERK 1/2,[38] whereas Snail and Slug decrease proliferation through the inhibition of Cyclin D2[39] and Cyclin D1.[40]

More interestingly, we also observed that SPARC regulates the *in vitro* migration and invasion of PCa cells. We found that SPARC knockdown decreased cell motility and invasion in PC3 cells, whereas overexpression of SPARC increased cell motility in LNCaP cells. These results show that SPARC not only acts as a paracrine chemoattractant, as previously reported,[14,15,41] but can also directly stimulates PCa migration and invasion in an autocrine manner. SPARC could, therefore, play a role in early tumor progression, in addition to the arrival of metastatic PCa cells to the bone.

CONCLUSION
Our data show that SPARC is highly-expressed in intermediate and high GS and induces EMT in PCa cells. In addition, SPARC induces PCa cell migration and invasion without affecting cell proliferation *in vitro*. These results indicate that SPARC regulates key events during tumor progression and therefore might play an important role in the

aggressiveness of PCa. Further molecular studies of the relationship between SPARC and Zeb1 should be conducted to better understand its contribution to tumor progression.

AUTHOR CONTRIBUTIONS

FLM designed and performed all the experiments and statistical analysis, and wrote the manuscript. MJT participated in experimental work and helped to draft the manuscript. EAC participated in the design and helped to draft the manuscript. HRC conceived the study, participated in its design and coordination, and helped to draft the manuscript. All authors read and approved the final manuscript.

COMPETING INTERESTS

All authors declare no competing interests.

REFERENCES

1. Ferlay J, Soerjomataram I, Ervik M, Dikshit R, Eser S, *et al*. GLOBOCAN v1.0. 2012: cancer incidence and mortality worldwide: IARC CancerBase No. 11. Lyon: International Agency for Research on Cancer; 2013. Available from: http://www.globocan.iarc.fr. [Last accessed on 17 Oct 2018].
2. American Society of Clinical Oncology. Prostate Cancer Statistics. American Society of Clinical Oncology; 2016. Available from: http://www.cancer.net/cancer-types/prostate-cancer/statistics. [Last accessed on 17 Oct 2018].
3. Sartor O, de Bono JS. Metastatic prostate cancer. *N Engl J Med* 2018; 378: 645–57.
4. Rosset E, Bradshaw A. SPARC/osteonectin in mineralized tissue. *Matrix Biol* 2015; 52–54: 78–87.
5. Bradshaw AD. The role of SPARC in extracellular matrix assembly. *J Cell Commun Signal* 2009; 3: 239–46.
6. Bradshaw A, Sage E. SPARC, a matricellular protein that functions in cellular differentiation and tissue response to injury. *J Clin Invest* 2001; 107: 1049–54.
7. Arnold S, Brekken R. SPARC: a matricellular regulator of tumorigenesis. *J Cell Commun Signal* 2009; 3: 255–73.
8. Sung SY, Chang JL, Chen KC, Yeh SD, Liu YR, *et al*. Co-targeting prostate cancer epithelium and bone stroma by human osteonectin-promoter-mediated suicide gene therapy effectively inhibits androgen-independent prostate cancer growth. *PLoS One* 2016; 11: e0153350.
9. Yusuf N, Inagaki T, Kusunoki S, Okabe H, Yamada I. SPARC was overexpressed in human endometrial cancer stem-like cells and promoted migration activity. *Gynecol Oncol* 2014; 134: 356–63.
10. Nagaraju GP, Dontula R, El-Rayes BF, Lakka SS. Molecular mechanisms underlying the divergent roles of SPARC in human carcinogenesis. *Carcinogenesis* 2014; 35: 967–73.
11. Ribeiro N, Sousa S, Brekken R, Monteiro F. Role of SPARC in bone remodeling and cancer-related bone metastasis. *J Cell Biochem* 2014; 115: 17–26.
12. Chong HC, Tan CK, Huang RL, Tan NS. Matricellular proteins: a sticky affair with cancers. *J Oncol* 2012; 2012: 351049.
13. Tai IT, Tang MJ. SPARC in cancer biology: its role in cancer progression and potential for therapy. *Drug Resist Updat* 2008; 11: 231–46.
14. De S, Chen J, Narizhneva NV, Heston W, Brainard J, *et al*. Molecular pathway for cancer metastasis to bone. *J Biol Chem* 2003; 278: 39044–50.
15. Jacob K, Webber M, Benayahu D, Kleinman H. Osteonectin promotes prostate cancer cell migration and invasion: a possible mechanism for metastasis to bone. *Cancer Res* 1999; 56: 4453–7.
16. Shin M, Mizokami A, Kim J, Ofude M, Konaka H, *et al*. Exogenous SPARC suppresses proliferation and migration of prostate cancer by interacting with integrin β1. *Prostate* 2013; 73: 1159–70.
17. Kapinas K, Lowther KM, Kessler CB, Tilbury K, Lieberman JR, *et al*. Bone matrix osteonectin limits prostate cancer cell growth and survival. *Matrix Biol* 2012; 31: 299–307.
18. Said N, Frierson HF, Chernauskas D, Conaway M, Motamed K, *et al*. The role of SPARC in the TRAMP model of prostate carcinogenesis and progression. *Oncogene* 2009; 28: 3487–98.
19. Fenouille N, Tichet M, Dufies M, Pottier A, Mogha A, *et al*. The epithelial-mesenchymal transition (EMT) regulatory factor SLUG (SNAI2) is a downstream target of SPARC and AKT in promoting melanoma cell invasion. *PLoS One* 2012; 7: e40378.
20. Hung J, Yen M, Jian S, Wu C, Chang W. Secreted protein acidic and rich in cysteine (SPARC) induces cell migration and epithelial mesenchymal transition through WNK1/snail in non-small cell lung cancer. *Oncotarget* 2017; 8: 63691–702.
21. Grant JL, Fishbein MC, Hong L, Krysan K, Minna JD, *et al*. A novel molecular pathway for snail-dependent, SPARC-mediated invasion in non–small cell lung cancer pathogenesis. *Cancer Prev Res* 2014; 7: 150–61.
22. Heerboth S, Housman G, Leary M, Longacre M, Byler S, *et al*. EMT and tumor metastasis. *Clin Transl Med* 2015; 4: 6.
23. Nieto MA, Huang RY, Jackson RA, Thiery JP. EMT: 2016. *Cell* 2016; 166: 21–45.
24. Dalla Pozza E, Forciniti S, Palmieri M, Dando I. Secreted molecules inducing epithelial-to-mesenchymal transition in cancer development. *Semin Cell Dev Biol* 2017; 78: 62-72.
25. Derosa CA, Furusato B, Shaheduzzaman S, Srikantan V, Wang Z, *et al*. Elevated osteonectin/SPARC expression in primary prostate cancer predicts metastatic progression. *Prostate Cancer Prostatic Dis* 2012; 15: 150–6.
26. Thomas R, True L, Bassuk J, Lange P, Vessella R. Differential expression of osteonectin/SPARC during human prostate cancer progression. *Clin Cancer Res* 2000; 6: 1140–9.
27. Chang CH, Yen MC, Liao SH, Hsu YL, Lai CS, *et al*. Secreted protein acidic and rich in cysteine (SPARC) enhances cell proliferation, migration, and epithelial mesenchymal transition, and SPARC expression is associated with tumor grade in head and neck cancer. *Int J Mol Sci* 2017; 18. pii: E1556.
28. Robichaud N, Del Rincon SV, Huor B, Alain T, Petruccelli LA, *et al*. Phosphorylation of eIF4E promotes EMT and metastasis via translational control of SNAIL and MMP-3. *Oncogene* 2014; 34: 2032–42.
29. Jiang H, Li T, Qu Y, Wang X, Li B, *et al*. Long non-coding RNA SNHG15 interacts with and stabilizes transcription factor Slug and promotes colon cancer progression. *Cancer Lett* 2018; 425: 78–87.
30. Sánchez-Tilló E, Liu Y, De Barrios O, Siles L, Fanlo L, *et al*. EMT-activating transcription factors in cancer: beyond EMT and tumor invasiveness. *Cell Mol Life Sci* 2012; 69: 3429–56.
31. Farfán N, Ocarez N, Castellón EA, Mejía N, de Herreros AG, *et al*. The transcriptional factor ZEB1 represses Syndecan 1 expression in prostate cancer. *Sci Rep* 2018; 8: 11467.
32. Guo W, Giancotti FG. Integrin signalling during tumour progression. *Nat Rev Mol Cell Biol* 2004; 5: 816–26.
33. Zhang P, Sun Y. ZEB1: at the crossroads of epithelial-mesenchymal transition, metastasis and therapy resistance. *Cell Cycle* 2015; 14: 481–7.
34. Zhang P, Wei Y, Wang L, Debeb BG, Yuan Y, *et al*. ATM-mediated stabilization of ZEB1 promotes DNA damage response and radioresistance through CHK1. *Nat Cell Biol* 2014; 16: 864–75.
35. Hanrahan K, Neill AO, Prencipe M, Bugler J, Murphy L, *et al*. The role of epithelial–mesenchymal transition drivers ZEB1 and ZEB2 in mediating docetaxel-resistant prostate cancer. *Mol Oncol* 2017; 11: 251–65.
36. Chen N, Ye XC, Chu K, Navone NM, Sage EH, *et al*. A secreted isoform of ErbB3 promotes osteonectin expression in bone and enhances the invasiveness of prostate cancer cells. *Cancer Res* 2007; 67: 6544–8.
37. Sharma S, Xing F, Liu Y, Wu K, Said N, *et al*. Secreted protein acidic and rich in cysteine (SPARC) mediates metastatic dormancy of prostate cancer in the bone. *J Biol Chem* 2016; 291: 19351–63.
38. Song X, Chang H, Liang Q, Guo Z, Wu J. ZEB1 promotes prostate cancer proliferation and invasion through ERK1/2 signaling pathway. *Eur Rev Med Pharmacol Sci* 2017; 21: 4032–8.
39. Vega S, Morales AV, Ocaña OH, Valdés F, Fabregat I, *et al*. Snail blocks the cell cycle and confers resistance to cell death. *Genes Dev* 2004; 18: 1131–43.
40. Liu J, Uygur B, Zhang Z, Shao L, Romero D, *et al*. Slug inhibits proliferation of human prostate cancer cells via downregulation of cyclin D1 expression. *Prostate* 2010; 70: 1768–77.
41. Mateo F, Meca-Cortés O, Celià-Terrassa T, Fernández Y, Abasolo I, *et al*. SPARC mediates metastatic cooperation between CSC and non-CSC prostate cancer cell subpopulations. *Mol Cancer* 2014; 13: 237.